

# Differential cross sections for $K^+ p$ elastic scattering from 0.865 to 2.125 GeV/c<sup>†</sup>

K. Abe,\* B. A. Barnett, J. H. Goldman,<sup>‡</sup> A. T. Laasanen,<sup>§</sup> and P. H. Steinberg  
*University of Maryland, College Park, Maryland 20742*

G. J. Marmer, D. R. Moffett, and E. F. Parker

*Argonne National Laboratory, Argonne, Illinois 60439*

(Received 5 October 1973; revised manuscript received 7 October 1974)

We report on an experiment to obtain differential cross sections for  $K^+ p$  elastic scattering in the vicinity of the possible exotic baryon, the  $Z_1^*(1900)$ . The differential cross sections are based on typically 70 000 selected events in the angular region  $-0.9 \leq \cos\theta_{c.m.} \leq 0.9$  at each of 22 momenta from 0.865 to 2.125 GeV/c. The data are intended for use in partial-wave analysis to search for the  $Z_1^*$ .

## I. INTRODUCTION

The possibility of the existence of exotic hadrons, i.e., meson and baryon states which cannot be constructed from quark products  $q\bar{q}$  and  $qqq$ , respectively, has attracted considerable attention. This is because of the paradoxical role that such particles would play.

Their nonexistence is supported by the success of quark models in classifying the low-lying baryon and meson states in schemes based upon  $qqq$  products for baryons<sup>1</sup> and  $q\bar{q}$  products for mesons.<sup>2</sup> These models do not, however, rule out states with  $q\bar{q}$  excitation presumably at higher energies. In addition, two-component duality along with the assumed absence of exotics has been used to explain the qualitative features of total cross sections at high energies.<sup>3</sup> The same considerations have been used to derive exchange-degeneracy constraints for Regge trajectories which have been moderately successful.<sup>4</sup> It must be stressed, however, that these conclusions would not be invalidated by the existence of exotics if the intercepts of their Regge trajectories are found to be much lower than those of the nonexotics.

On the other hand, strict application of duality requires the contribution of  $q\bar{q}q\bar{q}$  meson exchange to the elastic scattering  $B\bar{B} \rightarrow B\bar{B}$  of baryons and antibaryons.<sup>5</sup> Similar reasoning applied to the process  $B\bar{B}B \rightarrow B\bar{B}B$  requires the existence of  $qqq\bar{q}\bar{q}$  exotic baryon exchange.<sup>6</sup>

At the present time the best candidates for exotics are the  $Z_0^*$  and  $Z_1^*$  suggested by the bump structures of the  $I=0$  and  $I=1$   $K$ -nucleon cross sections.<sup>7</sup> A substantial effort has gone into the measurement and the partial-wave analysis of the elastic and inelastic scattering in the region of these bumps.<sup>8</sup> Although there are suggestions of resonance behavior, the results have been inconclusive.

The data are most abundant for  $K^+ p$  elastic scattering. However, the evidence is that the  $Z_1^*$  is both broad and inelastic, thereby making its detection difficult. More precise data and perhaps better methods of analysis are certainly required.

We describe in this report the measurement of the differential cross sections for elastic  $K^+ p$  scattering with high statistical precision. Measurements were made at 22 momenta between 0.865 and 2.125 GeV/c, generally at momenta where polarization data are available. These measurements were carried out in an experiment at the Argonne National Laboratory in which the differential cross sections for  $\pi^+ p$ ,<sup>9,10</sup>  $K^- p$ ,<sup>9</sup> and  $p p$  elastic scattering were also obtained.

A brief account of the experimental methods and data analysis is given in Sec. II. More detailed descriptions of the equipment and data analysis are given elsewhere.<sup>10,11</sup> The results are presented and discussed in Sec. III and the results of a partial-wave analysis<sup>12</sup> based in part on these data are given in Sec. IV. In this analysis a resonance pole is seen in the  $P_{3/2}$  partial-wave amplitude and this constitutes the best evidence to date for the existence of the  $Z_1^*$ .

## II. EXPERIMENTAL METHODS

In the experiment<sup>11</sup> kaons in a partially separated beam were selected from background particles by a combination of Čerenkov counters and time-of-flight measurement. Further details on the beam and the Čerenkov counters are given in Ref. 13 with the single modification of the beam for this experiment being a downstream displacement of the final focus  $F_2$  by six feet. The additional distance between  $F_2$  and the last quadrupole  $Q_7$  reduced the horizontal convergence from 70 mrad to 30 mrad, thereby producing a nearly constant beam profile over the length of the liquid hydrogen

target at  $F_2$ . The production target in the Zero Gradient Synchrotron external beam (EPB I) was copper with dimensions 3 in. long,  $\frac{1}{4}$  in. wide,  $\frac{1}{8}$  in. high.

The kaons were scattered in a 6 in. long and 1.5 in. diameter liquid hydrogen target, and both the scattered kaon and the recoil proton were detected in banks of scintillation counters and wire-plane spark chambers with magnetostrictive readout which flanked the target on the left- and right-hand sides of the beam line. Data from the counters and the spark chambers were read into an on-line computer, and elastic scattering events were selected on the basis of coplanarity and the angles of the reconstructed tracks with respect to the beam line. The precision of the track reconstruction enabled a unique determination of the center-of-mass scattering angle everywhere except in a small region around the crossover angle where both particles have the same laboratory momentum. The experimental setup is shown in Fig. 1. The momentum bite of the beam was 1.0% to 1.5% and the central momentum was known to within 0.3%. The particle ratios at the final beam focus varied over the full momentum range from  $\pi/K = 1$  to 40 and  $p/K = 0.6$  to 2.0. Backward-scattered particles were detected mainly on the left-hand side in a bank of five spark chambers and an eight-element counter hodoscope aligned parallel to the beam line. The forward-going particles were detected on the right-hand side where the spark chambers and counter hodoscope

were set at  $45^\circ$  to the beam line. In this arrangement a constant geometric detection efficiency of 23.5% was achieved over the range of scattering angles except in a substantial region around the crossover angle where the efficiency was doubled by the inclusion of reverse kinematic events (i.e., forward-going particles towards the left, etc.). The event trigger consisted of an incident kaon in coincidence with a signal from each scattering hodoscope.<sup>10,11</sup> Two downstream veto counters  $A_1$  and  $A_2$  were used to significantly reduce the trigger rate, which varied from 1 to 13 per beam burst over the course of the experiment. Up to four sparks for each coordinate of each spark chamber could be recorded, and up to four tracks could be reconstructed on each side with at least three sparks required along each track. Typically 70 000 events at each momentum survived fiducial cuts in the vertex coordinates and scattering angles within which the geometric efficiency was constant. These events were sorted into  $\cos\theta_{c.m.}$  bins and the differential cross sections were obtained from the bin populations by applying corrections for the inelastic background, geometric efficiency, decay and rescattering, target length and density, beam attenuation, trigger accidentals, high-voltage pulse efficiency, and the track recognition efficiency of the spark chambers. A combination of the errors in these corrections would produce a  $\pm 1.5\%$  error on the over-all normalization, which is the same for all momenta.

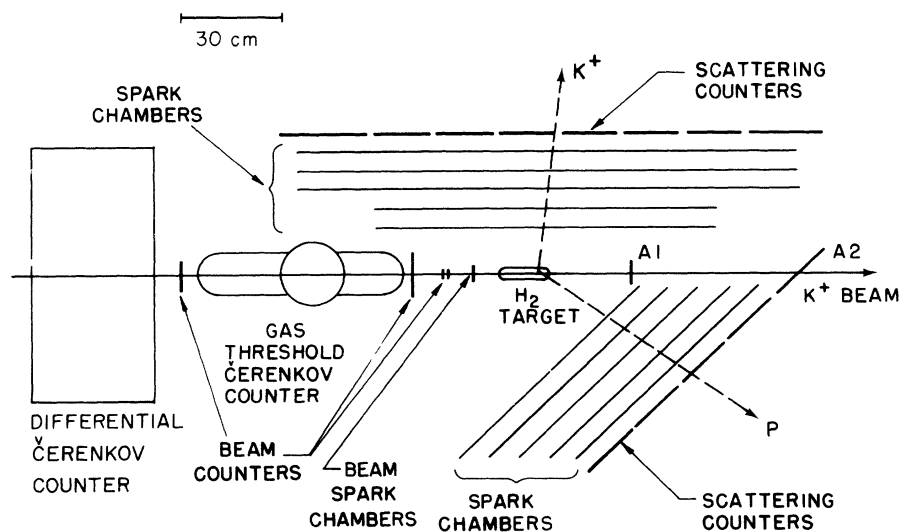


FIG. 1. Plan view of experimental apparatus.

The inefficiencies of individual spark chambers were determined from the numbers of missing sparks in reconstructed tracks and varied from 3% to 15%. The track recognition efficiencies were computed from these to be better than 99% assuming that the causes of spark failure were uncorrelated between individual spark chambers. Evidence that this assumption may not be valid for a small class of triggers was seen in fluctuations in  $\sigma_{\text{EL}}$  (the total elastic scattering cross sections) from different data runs at the same momentum. A single data run consisted of 5 000 to 10 000 events, and the fluctuations in  $\sigma_{\text{EL}}$  were sometimes greater than what could be explained by statistics alone. The value of  $\sigma_{\text{EL}}$  was found to be correlated with the instantaneous beam rate and the computed spark-chamber track recognition efficiency. However, the angular distributions from different data runs were consistent with each other. In order to correct for this effect the observed correlation between computed track recognition efficiency and  $\sigma_{\text{EL}}$  was used at each momentum to extrapolate to 100% efficiency. In this fashion the over-all normalization was increased by an amount which varied from  $(0 \pm 2.5)\%$  at the lowest momentum to  $(5.0 \pm 2.5)\%$  at the highest momentum where the beam rates were the greatest. The  $\pm 2.5\%$  error in this correction, which introduces a momentum-to-momentum uncertainty, is combined in quadrature with the errors from the other corrections to give a normalization error of  $\pm 3\%$ .

### III. RESULTS

The differential cross sections with their statistical errors are given in Table I. The main features of the data are illustrated in Fig. 2, where the data are plotted with smooth curves drawn to guide the eye.

A Legendre-polynomial fit was made to the data at each momentum of the form

$$\frac{d\sigma}{d\Omega}(\theta_{\text{cm}}, P_{\text{lab}}) = \frac{1}{k^2} \sum_{L=0} B_L(P_{\text{lab}}) P_L(\cos\theta_{\text{cm}}),$$

where the value  $N$  was chosen at each momentum by the following prescription:

(1)  $N$  was increased until the  $\chi^2/\text{NDF}$  of the fit failed to decrease by at least 25%, and

(2)  $N$  was forced to be at least as large as the value of  $N$  used in the previous (lower) momentum. The ratios  $B_L/B_0$  of the coefficients and their errors are given in Table II and plotted in Fig. 3 for the lower values of  $L$  along with the results

from the recent similar experiment of Charles *et al.*<sup>14</sup> The plotted points from the two experiments are consistent with each other, indicating general agreement in the shapes of the angular distributions. The values of  $\sigma_{\text{EL}}$ ,  $d\sigma/d\Omega(0)$ , and  $B$ , the slope parameter of the forward diffraction peak, are listed in Table III along with their statistical errors. The values of  $\sigma_{\text{EL}}$  were obtained from a Legendre-polynomial fitting, while  $d\sigma/d\Omega(0)$  (see Ref. 15) and  $B$  were derived from a fitting of the forward data to the formula  $d\sigma/dt = A \exp(Bt)$  in the interval  $t > -0.5$  (GeV/c)<sup>2</sup>.

The slope parameters are plotted in Fig. 4 along with values given by Charles *et al.*,<sup>14</sup> and the good agreement between the results of the two experiments is further evidence for the consistency of the angular distributions. However, there is a clear discrepancy in normalization between the two experiments, as seen in Fig. 5 in which the values for  $\sigma_{\text{EL}}$  are plotted along with some values from bubble-chamber experiments.<sup>16,17</sup> One finds agreement in normalization with the BGRT bubble-chamber experiment<sup>17</sup> but the results of Charles *et al.*<sup>14</sup> are, on the average, seven percent greater than our own, and this discrepancy is just beyond the quoted errors in the two experiments.

A possible check on our normalization would be the comparison of our extrapolated  $d\sigma/d\Omega(0)$  with the results of calculations based on forward dispersion relations. We have considered for this purpose the recent calculation of Baillon *et al.*<sup>18</sup> which uses the measured values of the real parts of the forward  $K^+ p$  scattering amplitudes obtained in a Coulomb interference experiment by the same group.<sup>19</sup> The data are plotted in Fig. 6 along with smooth curves representing the upper and lower standard deviation limits based on total cross sections<sup>7</sup> and the results of Ref. 18. Our data are in satisfactory agreement with these predictions.

### IV. DISCUSSION

As a preliminary step in a phase-shift analysis, solutions were found at twelve momenta up to 1.6 GeV/c.<sup>20</sup> It is characteristic of such analyses based upon earlier data that the solutions lie in distinct groups on the Argand diagrams of the partial-wave amplitudes.<sup>20-22</sup> It was of particular interest to see what might be the effect of these high-precision differential cross section data upon the locations and sizes of these groups. In the analysis, amplitudes up to  $l=4$  were varied, while the remaining amplitudes up to  $l=8$  were those of Lovelace and Wagner<sup>23</sup> based upon a Regge fit to

TABLE I.  $K^+p$  elastic differential cross sections (DCS) and errors ( $\Delta$ ) in microbarns per steradian.

$P_{K^+}$ (GeV/c) $\cos\theta$	0.865		0.910		0.970		1.098		1.170		1.207	
	DCS	$\Delta$										
0.8625							1647	55	1954	59	2148	53
0.8375							1637	55	1901	59	2069	51
0.8125			1128	57	1380	75	1533	52	1808	57	1960	51
0.7875	1007	60	1053	57	1299	73	1557	52	1781	57	1853	50
0.7625	1077	62	1100	57	1249	73	1481	52	1566	54	1764	47
0.7375	1002	60	1061	57	1187	70	1451	50	1618	54	1644	46
0.7125	1082	62	1153	57	1147	70	1394	50	1563	54	1573	45
0.6875	980	60	1083	57	1172	70	1258	47	1465	51	1551	46
0.6625	900	57	1011	55	1100	68	1180	45	1395	48	1487	45
0.6375	965	60	932	51	1078	68	1248	47	1300	48	1497	45
0.6125	918	57	950	51	1064	68	1177	45	1225	46	1402	45
0.5875	935	58	976	55	1026	66	1184	47	1193	46	1339	41
0.5625	1042	63	970	55	1013	66	1190	48	1202	46	1324	41
0.5375	782	53	932	53	932	64	1094	45	1157	46	1240	40
0.5125	962	61	938	53	965	64	1014	43	1104	44	1149	40
0.4875	932	58	890	38	944	64	988	43	1092	44	1079	39
0.4625	864	41	881	38	939	44	1026	30	964	41	1033	27
0.4375	911	42	870	36	895	45	935	29	933	30	957	26
0.4125	914	43	888	38	861	43	898	28	932	30	918	25
0.3875	903	42	918	38	849	43	940	29	1001	31	935	25
0.3625	868	41	811	35	870	44	840	27	876	29	888	25
0.3375	883	41	857	36	937	44	850	28	850	28	851	25
0.3125	896	43	824	38	850	45	830	28	862	29	807	24
0.2875	929	43	826	38	879	46	839	29	809	30	777	24
0.2625	935	44	852	38	818	44	771	28	803	29	780	24
0.2375			828	38	785	44	736	28	748	28	785	25
0.1750	849	40	828	36								
0.1625					829	34	703	21				
0.1500									662	24	634	20
0.0875	819	42	806	38	755	44						
0.0625	927	44	804	38	757	43	695	27	599	25	463	21
0.0375	833	43	755	36	747	43	654	27	566	25	527	21
0.0125	854	41	807	38	809	44	608	28	607	27	539	21
-0.0125	868	40	820	35	760	41	594	25	525	25	486	20
-0.0375	813	39	733	33	723	40	575	24	539	23	500	20
-0.0625	793	39	810	34	736	40	586	24	504	23	498	19
-0.0875	804	38	704	33	691	38	546	23	506	23	464	20
-0.1125	784	39	769	33	658	37	559	23	462	22	466	19
-0.1375	744	37	754	34	721	39	561	23	447	21	445	19
-0.1625	824	39	806	35	709	40	551	23	442	21	413	18
-0.1875	793	38	848	35	628	36	534	23	434	21	439	18
-0.2125	863	40	787	33	697	39	544	23	433	21	400	17
-0.2375	801	38	752	33	710	39	519	23	428	21	380	17
-0.2625	846	40	793	34	715	39	530	23	417	29	362	16
-0.2875	858	56	766	46	763	56	529	32	442	29	377	18
-0.3125	876	54	749	46	645	52	505	32	419	29	383	22
-0.3375	885	54	776	46	741	57	525	31	386	25	401	23
-0.3625	893	54	803	48	744	56	498	29	449	28	371	24
-0.3875	919	57	854	48	701	54	515	32	404	28	391	22
-0.4125	840	54	791	49	745	56	484	29	407	28	361	22
-0.4375	868	55	770	47	670	52	461	29	422	28	363	22
-0.4625	964	57	840	49	730	54	523	31	340	26	366	23
-0.4875	912	55	820	49	775	56	597	32	415	28	382	23
-0.5125	784	52	804	46	730	54	567	32	413	28	371	22
-0.5375	950	57	896	48	771	57	549	32	423	28	367	22
-0.5625	952	58	935	51	769	57	505	29	426	28	383	22
-0.5875	858	55	910	53	779	57	573	32	384	26	417	24
-0.6125	997	58	946	53	754	57	596	32	421	28	388	22

TABLE I. (Continued)

$P_{K^+}$ (GeV/c) $\cos\theta$	0.865		0.910		0.970		1.098		1.170		1.207	
	DCS	$\Delta$										
-0.6375	944	58	922	53	870	59	529	32	441	29	413	24
-0.6625	1050	60	941	51	861	59	564	32	453	29	403	23
-0.6875	1040	61	973	53	878	59	586	31	511	31	403	23
-0.7125	1106	60	961	54	930	62	601	32	487	28	431	24
-0.7375	924	55	1060	56	928	62	678	35	465	28	477	24
-0.7625	1139	60	1017	53	830	58	649	35	505	31	464	25
-0.7875	1064	61	1099	57	1010	66	679	35	498	29	442	24
-0.8125	1032	59	1103	57	1051	66	729	35	607	32	506	26
-0.8375	1210	66	1029	54	1042	67	748	35	542	32	520	25
-0.8625	1238	66	1109	56	1019	64	710	36	591	32	493	26
-0.8875	1154	62	1114	57	983	64	735	35	637	32	515	26
-0.9125	1171	66	1185	58	1099	67	747	36				
$P_{K^+}$ (GeV/c) $\cos\theta$	1.255		1.310		1.370		1.400		1.450		1.495	
	DCS	$\Delta$										
0.8875			2396	63	2404	58	2551	63	2353	59	2581	61
0.8625	2113	84	2260	60	2212	58	2299	59	2174	57	2377	58
0.8375	1996	82	2125	58	2129	56	2174	57	2107	57	2128	56
0.8125	1892	79	2015	58	2094	56	2141	57	1988	53	1973	52
0.7875	1877	79	1974	58	1909	53	2049	57	1894	53	2057	52
0.7625	1796	79	1821	55	1811	51	1928	54	1796	51	1825	50
0.7375	1574	75	1755	52	1721	51	1771	52	1676	48	1670	47
0.7125	1666	77	1654	52	1747	51	1624	49	1653	48	1661	47
0.6875	1513	71	1555	50	1604	49	1548	49	1474	46	1478	45
0.6625	1472	71	1553	50	1474	49	1546	49	1441	46	1397	45
0.6375	1375	69	1471	50	1449	45	1330	47	1341	46	1411	45
0.6125	1423	69	1373	46	1311	45	1348	47	1339	46	1298	42
0.5875	1447	71	1305	46	1352	45	1178	44	1147	40	1156	40
0.5625	1283	66	1213	44	1160	43	1172	44	1182	44	1238	42
0.5375	1303	66	1238	44	1143	43	1086	41	1166	40	1082	40
0.5125	1136	64	1127	44	1098	40	966	41	1029	40	1047	40
0.4875	1136	64	1118	44	1030	40	943	39	943	38	976	37
0.4625	1121	64	1037	41	998	40	902	39	928	38	929	37
0.4375	1019	42	1023	42	937	38	743	35	925	38	864	34
0.4125	980	43	960	29	871	38	822	25	840	35	800	34
0.3875	949	41	974	29	901	27	821	26	791	35	808	25
0.3625	884	39	881	28	804	25	772	26	772	24	771	24
0.3375	859	38	865	28	767	25	728	25	732	23	741	24
0.3125	874	39	789	27	740	25	691	24	717	24	682	22
0.2875	862	39	753	27	710	25	666	24	639	23	721	24
0.2625	722	37	712	25	690	24	652	24	625	23	663	22
0.2375	682	37	707	25			568	23	595	22	600	21
0.1500	639	32	599	22			560	16	502	17	496	16
0.1375											472	16
0.0625	604	37										
0.0375	561	36	510	24	436	21	380	20	415	20	411	20
0.0125	537	35	472	21	424	21	376	20	387	21	396	19
-0.0125	506	35	463	23	450	21	389	20	393	20	347	20
-0.0375	480	32	444	20	369	21	386	20	376	19	350	19
-0.0625	430	29	463	19	403	18	367	21	369	17	356	18
-0.0875	421	28	448	19	387	17	326	18	329	16	328	16
-0.1125	452	29	395	19	365	17	327	18	348	17	308	15
-0.1375	455	30	385	18	344	17	279	17	291	15	299	15
-0.1625	419	29	390	19	333	16	280	16	279	22	281	15
-0.1875	418	29	363	18	341	17	264	16	277	22	271	15
-0.2125	381	27	323	18	295	15	281	16	242	19	258	15
-0.2375	343	26	330	24	289	21	242	22	244	21	243	18
-0.2625	316	34	318	24	252	21	250	22	248	19	220	18

TABLE I. (*Continued*)

$P_{K^+}$ (GeV/c) $\cos\theta$	1.255		1.310		1.370		1.400		1.450		1.495	
	DCS	$\Delta$										
-0.2875	354	36	322	24	269	21	278	22	236	19	233	18
-0.3125	302	34	293	21	265	21	219	19	241	19	211	18
-0.3375	324	34	312	21	230	18	245	19	218	19	188	18
-0.3625	361	37	313	21	222	18	235	19	218	19	205	18
-0.3875	297	35	292	21	246	21	203	19	185	16	146	15
-0.4125	328	35	273	21	217	18	175	19	189	19	180	15
-0.4375	266	32	278	21	246	18	201	19	189	19	176	16
-0.4625	297	35	300	21	216	18	182	19	175	16	167	15
-0.4875	367	36	289	21	200	18	239	19	192	19	169	15
-0.5125	306	34	276	21	203	18	220	19	169	16	166	15
-0.5375	338	35	265	21	227	18	181	17	171	16	188	16
-0.5625	293	31	277	21	217	18	186	17	163	16	141	15
-0.5875	295	35	239	19	247	18	203	19	165	16	160	16
-0.6125	340	34	292	21	230	18	176	17	176	16	144	15
-0.6375	306	31	251	21	216	18	174	17	166	15	181	16
-0.6625	370	37	298	21	227	18	200	19	164	15	159	15
-0.6875	363	34	281	21	241	18	185	17	143	15	182	15
-0.7125	369	34	294	21	230	18	212	19	159	16	184	15
-0.7375	327	34	299	21	249	18	220	19	201	19	182	16
-0.7625	381	37	304	22	248	18	194	17	180	15	174	16
-0.7875	384	37	338	22	288	22	212	19	172	16	152	16
-0.8125	399	37	327	22	283	22	235	19	193	15	192	16
-0.8375	390	38	391	25	294	19	226	20	188	16	192	15
-0.8625	507	41	379	25	283	19	288	20	207	16	193	16
-0.8875	417	35	397	25	290	19	233	20	224	20	178	16
$P_{K^+}$ (GeV/c) $\cos\theta$	1.540		1.600		1.640		1.705		1.740		1.790	
	DCS	$\Delta$										
0.9125			2646	50	2781	57	3015	62	2955	63	2865	62
0.8875	2475	56	2489	50	2595	55	2780	62	2773	61	2508	57
0.8625	2167	54	2371	47	2325	53	2521	56	2610	58	2344	55
0.8375	2167	54	2212	47	2165	52	2287	54	2308	55	2118	53
0.8125	2103	53	2050	45	1951	50	2082	51	2150	52	1960	52
0.7875	1906	51	1916	44	1867	47	2006	51	1916	50	1869	50
0.7625	1800	48	1741	42	1724	47	1817	48	1772	50	1715	48
0.7375	1684	48	1724	42	1627	44	1696	48	1704	46	1499	45
0.7125	1547	46	1564	38	1446	42	1550	46	1439	44	1431	44
0.6875	1541	46	1462	37	1476	42	1472	43	1390	44	1315	41
0.6625	1554	46	1373	37	1373	42	1329	43	1319	42	1211	40
0.6375	1378	41	1312	36	1228	38	1236	36	1165	38	1064	38
0.6125	1295	41	1186	36	1168	38	1091	37	1091	38	1028	38
0.5875	1180	39	1150	33	1094	36	1118	37	1035	36	950	35
0.5625	1025	37	1030	32	1045	36	1009	35	952	36	958	35
0.5375	1041	37	1036	33	923	33	1021	37	855	33	861	34
0.5125	988	37	945	31	940	33	871	35	775	33	760	32
0.4875	930	37	875	30	838	33	857	35	713	31	719	31
0.4625	882	37	795	28	796	30	728	32	663	31	657	30
0.4375	803	33	802	28	731	30	682	32	621	31	586	29
0.4125	840	33	742	27	716	30	705	32	599	27	632	29
0.3875	743	22	729	20	658	28	634	30	562	28	495	27
0.3625	736	22	675	19	622	20	554	20	511	19	506	27
0.3375	702	22	634	18	588	20	532	20	501	19	486	19
0.3125	678	21	643	19	578	20	547	20	447	18	440	19

TABLE I. (Continued)

$P_{K^+}$ (GeV/c) $\cos\theta$	1.540		1.600		1.640		1.705		1.740		1.790	
	DCS	$\Delta$										
0.2875	607	21	573	19	494	19	488	20	386	18	419	18
0.2625	570	21	539	18	489	18	446	19	382	17	384	18
0.2375	553	21	509	18	463	18	395	18	339	16	338	16
0.2125			464	16	435	17	412	18	330	16	336	16
0.1875	448	15										
0.1250			364	18	347	14	303	13	262	14	234	12
0.0125	370	18	337	15	300	17	228	14	206	14		
-0.0125	321	17	319	15	285	16	240	15	202	14	203	13
-0.0375	318	16	276	14	247	16	230	15	162	12	184	15
-0.0625	303	15	295	14	252	16	192	15	158	12	168	15
-0.0875	294	15	264	13	221	14	181	15	176	12	157	13
-0.1125	282	15	264	12	223	14	195	13	152	14	141	12
-0.1375	276	15	227	12	214	12	192	13	146	10	137	11
-0.1625	233	13	219	11	208	12	177	12	133	9	114	10
-0.1875	234	13	219	12	167	17	164	12	119	9	143	15
-0.2125	244	13	187	12	162	17	149	17	102	14	100	13
-0.2375	206	17	173	14	137	14	151	17	116	14	82	12
-0.2625	214	17	172	13	152	14	126	17	114	14	102	13
-0.2875	230	17	155	14	126	14	137	17	97	14	85	12
-0.3125	171	15	161	14	137	14	116	13	84	11	99	12
-0.3375	178	16	170	14	139	14	119	13	107	14	95	12
-0.3625	151	15	138	14	115	14	146	17	88	14	66	11
-0.3875	184	17	137	13	119	14	123	17	81	11	90	12
-0.4125	152	14	136	14	107	14	109	13	86	14	83	12
-0.4375	152	15	143	12	122	14	91	13	88	14	69	12
-0.4625	150	15	118	12	108	14	110	13	64	11	77	12
-0.4875	144	15	113	12	127	14	75	13	72	14	78	12
-0.5125	139	15	119	12	108	14	91	13	81	14	87	12
-0.5375	128	15	132	13	108	14	99	13	94	14	60	11
-0.5625	118	11	108	12	104	14	113	13	75	10	80	12
-0.5875	101	13	108	12	107	14	78	14	68	11	66	11
-0.6125	136	15	107	12	103	11	102	14	85	11	76	12
-0.6375	145	15	114	12	97	11	95	14	66	10	73	11
-0.6625	120	13	126	12	124	14	98	13	83	11	88	12
-0.6875	144	15	102	11	107	14	81	13	110	14	82	12
-0.7125	140	14	134	12	113	14	117	13	128	14	80	11
-0.7375	142	15	132	12	131	14	131	13	96	14	76	11
-0.7625	150	15	123	12	91	11	106	13	96	14	88	12
-0.7875	131	15	145	12	125	14	120	13	111	14	102	12
-0.8125	124	14	148	12	121	14	120	13	93	11	94	12
-0.8375	150	15	142	12	128	14	140	13	131	14	99	12
-0.8625	164	15	148	12	143	15	132	14	109	11	121	13
-0.8875	157	15	130	12	158	15	149	14	153	15	133	15
$P_{K^+}$ (GeV/c) $\cos\theta$	1.880		1.965		2.050		2.125					
	DCS	$\Delta$										
0.9125	3289	65	3003	57								
0.8875	2797	58	2601	52	2625	48	2486	56				
0.8625	2535	55	2420	52	2279	47	2179	54				
0.8375	2340	54	2121	46	2027	44	2027	50				
0.8125	2046	52	1864	44	1783	41	1779	49				
0.7875	1856	48	1682	44	1604	40	1498	47				
0.7625	1676	46	1524	40	1352	35	1374	43				
0.7375	1602	46	1355	38	1251	35	1260	43				
0.7125	1492	44	1276	38	1133	34	1096	41				
0.6875	1333	43	1104	36	1030	32	992	37				

TABLE I. (*Continued*)

$P_{K^+}$ (GeV/c)	1.880		1.965		2.050		2.125	
	$\cos\theta$	DCS	$\Delta$	DCS	$\Delta$	DCS	$\Delta$	DCS
0.6625	1195	38	1018	32	952	30	885	35
0.6375	1082	36	904	30	848	28	782	32
0.6125	991	36	848	30	799	28	691	32
0.5875	887	31	832	30	703	27	581	29
0.5625	832	32	720	27	634	25	538	29
0.5375	765	31	604	25	533	22	464	26
0.5125	688	29	573	25	526	22	429	26
0.4875	673	29	480	25	473	22	399	23
0.4625	595	29	447	21	401	20	364	23
0.4375	608	29	399	21	383	20	316	20
0.4125	459	26	412	22	358	20	292	20
0.3875	460	26	354	19	332	18	251	20
0.3625	458	22	293	19	273	18	274	20
0.3375	376	16	309	19	264	13	209	18
0.3125	364	16	259	12	241	11	195	13
0.2875	347	16	265	13	223	11	169	13
0.2625	288	15	223	12	178	11	148	11
0.2375	267	15	189	12	169	10	145	11
0.2125	258	15	192	12	153	9		
0.1125	180	10	133	8	105	7	81	7
0.0125			109	9				
-0.0125	148	12	101	9	83	8		
-0.0375	136	12	87	9	65	8	59	10
-0.0625	127	12	88	9	73	8	66	10
-0.0875	123	12	81	9	59	8	61	10
-0.1125	112	11	84	9	63	9	75	10
-0.1375	103	10	74	8	68	8	73	10
-0.1625	108	10	59	10	62	10	55	18
-0.1875	114	12	52	8	49	10	46	12
-0.2125	81	12	52	8	52	10	46	12
-0.2375	59	10	47	8	43	10	35	8
-0.2625	72	13	47	8	32	8	35	12
-0.2875	68	13	43	8	32	9	32	8
-0.3125	58	13	45	8	24	7	28	8
-0.3375	46	10	32	11	21	7	30	8
-0.3625	56	10	52	11	41	10	25	8
-0.3875	45	10	30	11	29	8	28	8
-0.4125	68	12	52	11	20	8	41	12
-0.4375	40	12	45	8	28	9	30	8
-0.4625	49	10	28	8	29	8	23	8
-0.4875	47	10	43	8	30	8	30	8
-0.5125	50	10	43	8	21	7	31	8
-0.5375	59	13	55	11	26	8	23	8
-0.5625	49	12	43	8	41	10	34	8
-0.5875	64	12	38	8	28	7	34	12
-0.6125	66	12	57	10	36	8	34	12
-0.6375	53	12	29	8	40	9	29	8
-0.6625	72	12	48	8	24	7	36	8
-0.6875	62	12	41	8	30	8	29	8
-0.7125	52	10	46	8	44	8	40	12
-0.7375	94	13	54	8	35	8	36	8
-0.7625	73	10	56	8	44	7	34	8
-0.7875	102	13	71	11	56	8	66	12
-0.8125	82	13	62	8	59	8	50	8
-0.8375	110	13	80	11	60	10	50	8
-0.8625	96	12	95	11	57	8	78	12
-0.8875	111	12	97	11	58	8	76	12

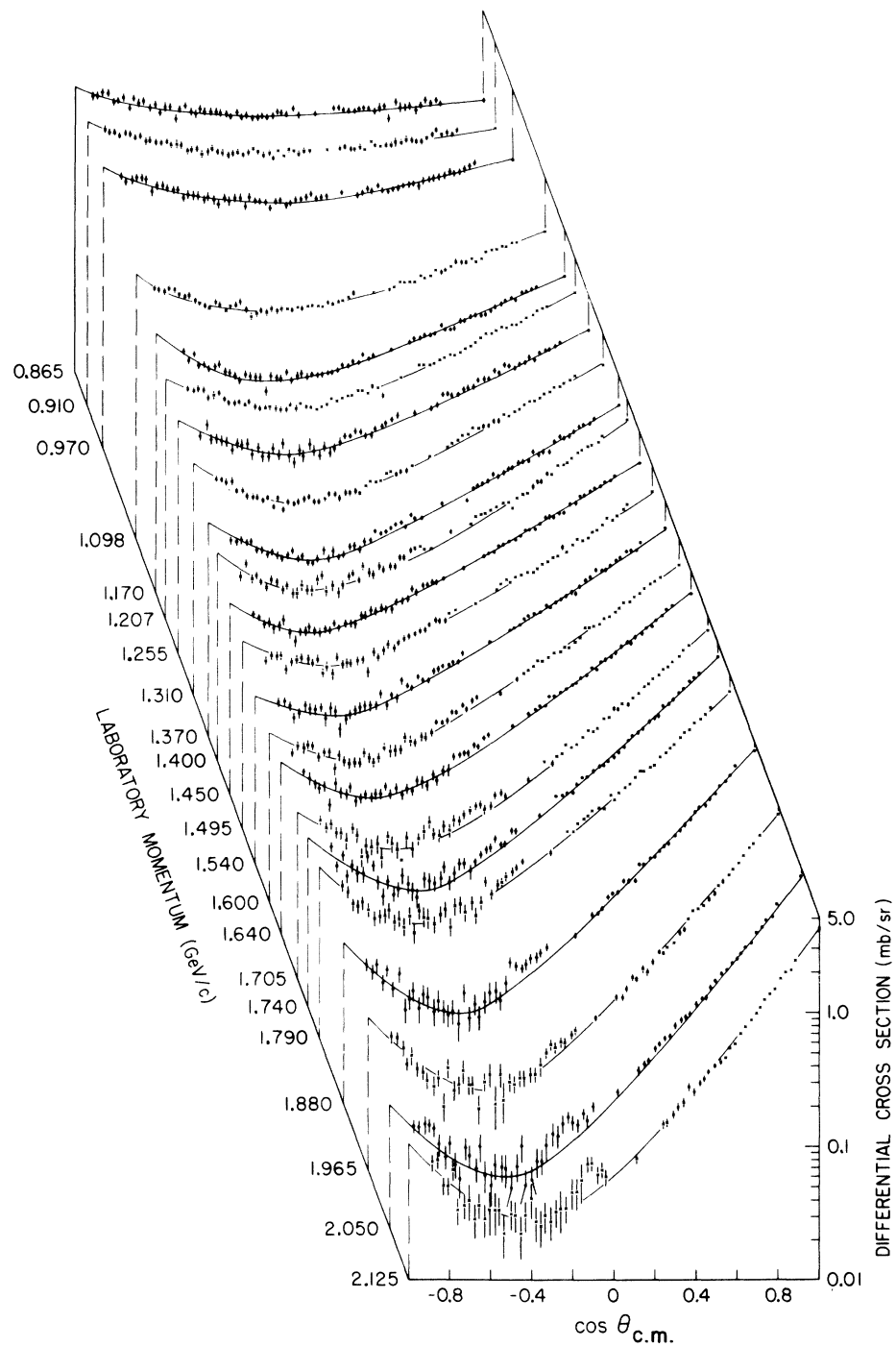


FIG. 2. Isometric plot of differential cross sections versus  $\cos \theta_{\text{c.m.}}$  and laboratory momentum.

TABLE II. Legendre polynomial coefficients.

Momentum (GeV/c)	$B_1/B_0$	$B_2/B_0$	$B_3/B_0$	$B_4/B_0$	$B_5/B_0$	$B_6/B_0$
0.865	-0.004 ± 0.020	0.278 ± 0.028				
0.910	0.055 ± 0.017	0.351 ± 0.024				
0.970	0.222 ± 0.020	0.444 ± 0.028				
1.098	0.602 ± 0.013	0.596 ± 0.016				
1.170	0.879 ± 0.017	0.730 ± 0.018	0.060 ± 0.019			
1.207	1.025 ± 0.016	0.847 ± 0.017	0.176 ± 0.017			
1.255	1.109 ± 0.023	0.785 ± 0.024	0.095 ± 0.025			
1.310	1.226 ± 0.016	0.944 ± 0.020	0.221 ± 0.018	0.134 ± 0.018		
1.370	1.346 ± 0.016	1.017 ± 0.020	0.284 ± 0.017	0.139 ± 0.017		
1.400	1.452 ± 0.017	1.155 ± 0.021	0.425 ± 0.018	0.204 ± 0.017		
1.450	1.462 ± 0.017	1.066 ± 0.022	0.351 ± 0.017	0.172 ± 0.018		
1.495	1.544 ± 0.019	1.143 ± 0.021	0.497 ± 0.026	0.242 ± 0.021	0.124 ± 0.022	
1.540	1.589 ± 0.020	1.189 ± 0.021	0.473 ± 0.026	0.224 ± 0.021	0.043 ± 0.022	
1.600	1.653 ± 0.020	1.300 ± 0.021	0.594 ± 0.026	0.295 ± 0.021	0.112 ± 0.022	
1.640	1.717 ± 0.016	1.409 ± 0.018	0.676 ± 0.020	0.325 ± 0.022	0.115 ± 0.018	
1.705	1.786 ± 0.016	1.565 ± 0.018	0.804 ± 0.022	0.382 ± 0.018	0.114 ± 0.018	
1.740	1.874 ± 0.017	1.725 ± 0.020	0.947 ± 0.023	0.455 ± 0.017	0.153 ± 0.018	
1.790	1.861 ± 0.018	1.669 ± 0.020	0.881 ± 0.023	0.412 ± 0.018	0.139 ± 0.019	
1.880	1.982 ± 0.023	1.948 ± 0.025	1.147 ± 0.027	0.589 ± 0.020	0.188 ± 0.019	
1.965	2.061 ± 0.019	2.168 ± 0.025	1.370 ± 0.023	0.817 ± 0.027	0.298 ± 0.018	0.118 ± 0.017
2.050	2.139 ± 0.020	2.230 ± 0.026	1.484 ± 0.025	0.835 ± 0.027	0.336 ± 0.019	0.091 ± 0.017
2.125	2.152 ± 0.023	2.358 ± 0.031	1.616 ± 0.028	0.981 ± 0.031	0.360 ± 0.021	0.120 ± 0.020

TABLE III. Total elastic and forward cross sections and slope of the forward diffraction peak.

Momentum (GeV/c)	Elastic cross section (millibarns)	$\frac{d\sigma}{d\Omega} (\theta = 0^\circ)$ (millibarns/ steradian)	"B," the forward diffraction peak slope [ $(\text{GeV}/c)^{-2}$ ]
0.865	11.98 ± 0.21	1.052 ± 0.027	0.54 ± 0.08
0.910	11.75 ± 0.21	1.166 ± 0.025	0.91 ± 0.07
0.970	11.62 ± 0.20	1.431 ± 0.036	1.42 ± 0.09
1.098	10.75 ± 0.19	1.971 ± 0.035	2.04 ± 0.06
1.170	10.55 ± 0.18	2.373 ± 0.051	2.26 ± 0.07
1.207	10.69 ± 0.19	2.763 ± 0.048	2.52 ± 0.05
1.255	10.32 ± 0.18	2.613 ± 0.060	2.16 ± 0.07
1.310	10.40 ± 0.18	2.869 ± 0.040	2.31 ± 0.04
1.370	9.83 ± 0.17	3.011 ± 0.049	2.42 ± 0.05
1.400	9.51 ± 0.17	3.412 ± 0.084	2.71 ± 0.17
1.450	9.17 ± 0.16	2.990 ± 0.057	2.35 ± 0.06
1.495	9.35 ± 0.16	3.195 ± 0.084	2.41 ± 0.08
1.540	8.79 ± 0.15	3.170 ± 0.096	2.40 ± 0.09
1.600	8.55 ± 0.15	3.270 ± 0.075	2.46 ± 0.05
1.640	8.35 ± 0.15	3.420 ± 0.070	2.55 ± 0.07
1.705	8.46 ± 0.15	3.891 ± 0.073	2.75 ± 0.06
1.740	8.04 ± 0.14	3.999 ± 0.076	2.84 ± 0.06
1.790	7.56 ± 0.13	3.741 ± 0.075	2.76 ± 0.05
1.880	7.36 ± 0.13	4.230 ± 0.121	2.96 ± 0.09
1.965	6.72 ± 0.12	4.281 ± 0.075	3.12 ± 0.06
2.050	6.19 ± 0.11	4.222 ± 0.102	3.13 ± 0.08
2.125	5.96 ± 0.10	4.229 ± 0.088	3.07 ± 0.07

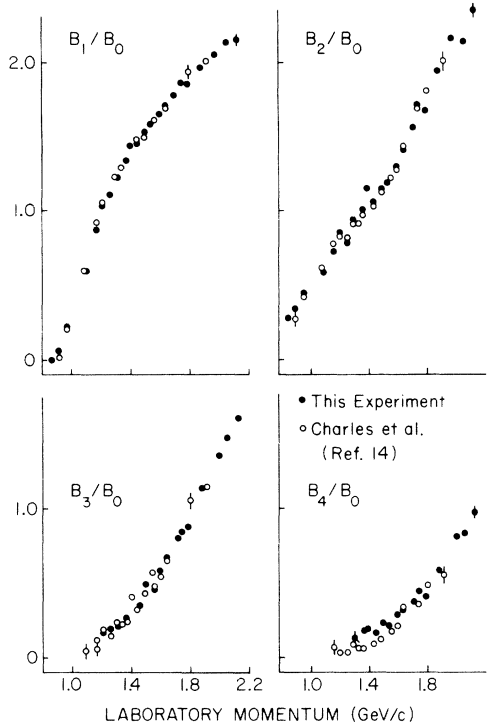


FIG. 3. Ratios of  $B_L/B_0$  of the coefficients of the expansion of  $d\sigma/d\Omega$  in Legendre polynomials.

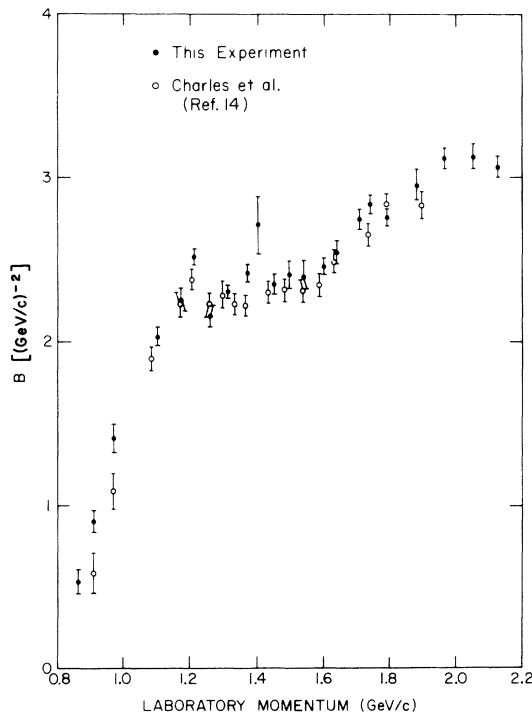


FIG. 4. Forward slope parameter  $B$  from the fitting of the differential cross sections to the formula  $d\sigma/dt = A \exp(Bt)$  for  $t > -0.05 (\text{GeV}/c)^2$ .

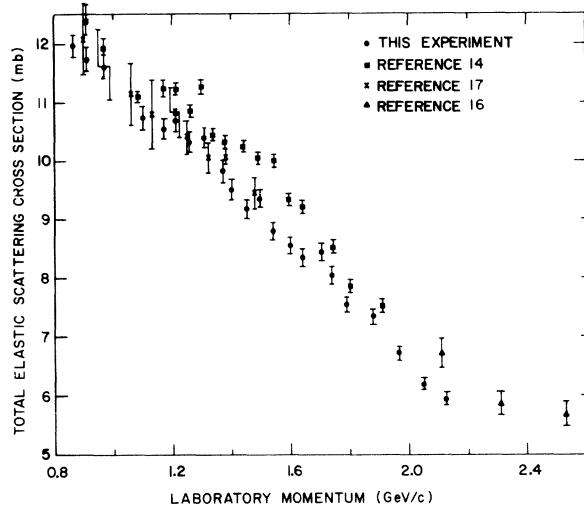


FIG. 5. Total elastic scattering cross section.

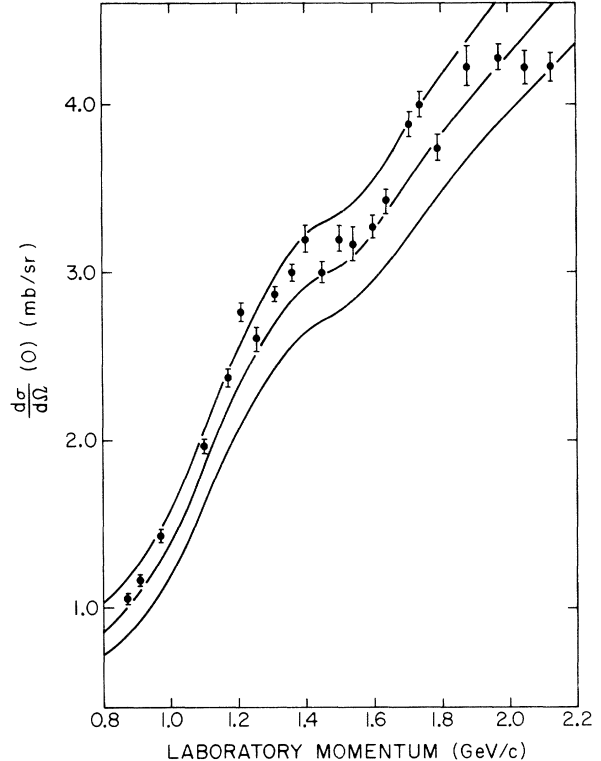


FIG. 6. Extrapolated  $d\sigma/d\Omega(0)$  in comparison with prediction based on total cross sections and forward dispersion relations. The smooth curves represent the upper and lower standard deviation limits.

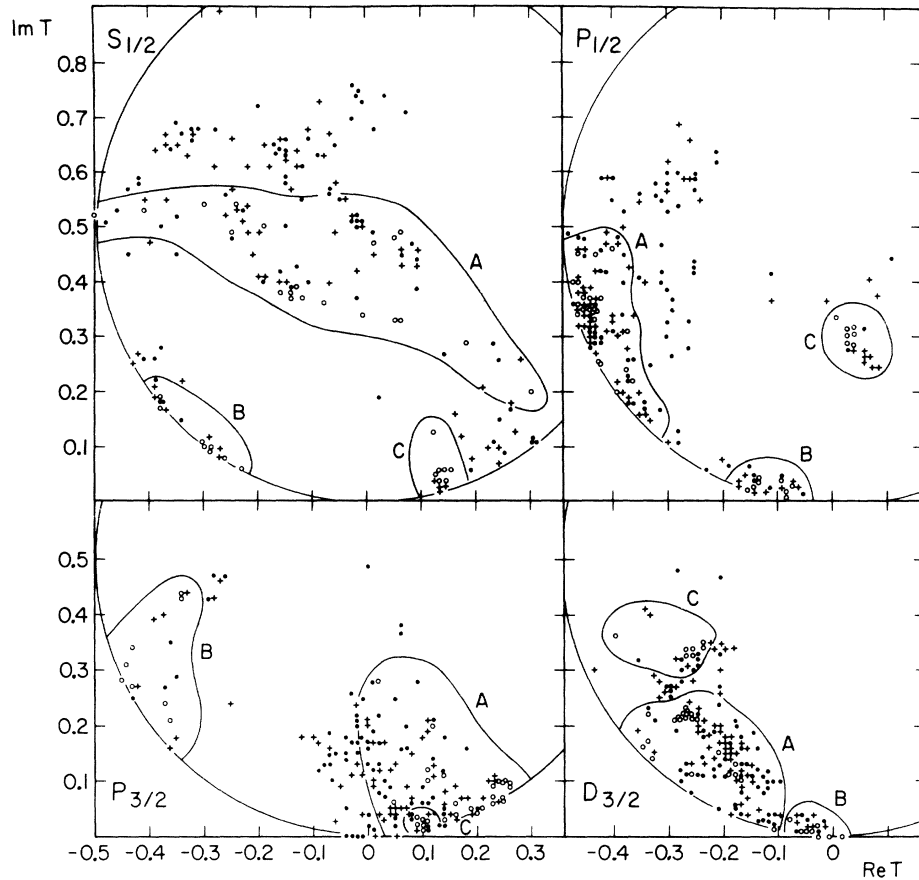


FIG. 7. Phase-shift analysis solutions at 1.54 GeV/c. The confidence levels for the solutions are indicated as follows:  $\circ$ , greater than 20%;  $+$ , in the interval 10%–20%;  $\cdot$ , in the interval 1%–10%.

higher-energy data. Searches for solutions were initiated in the vicinity of published solutions.<sup>20,22,23</sup> At the lowest momentum, where the inelastic cross section is relatively small, the solutions are tightly clustered at a single point representing the uniquely determined scattering state. At higher momenta, where the inelastic channels are more important, we find the solutions are distributed over wide regions of the Argand diagrams. The situation at 1.54 GeV/c is shown in Fig. 7, where 207 solutions with confidence levels greater than 1% obtained in 354 searches are plotted for the lower angular momentum states. An attempt was made to associate these solutions into smaller groups by examining the distribution of distances between pairs of solutions.<sup>20</sup> Only for those solutions with confidence levels greater than 20% ( $\chi^2/NDF = 112/100$ ) was it possible to define clearly separated groups, and the boundaries of these

groups *A*, *B*, and *C* are drawn in the figure. These results are similar to those of Ref. 22 in that these authors find no tendency to form groups above 1.5 GeV/c.

No attempts were made to obtain Argand trajectories using the shortest-path method. In fact, the validity of this and similar methods for selecting single energy solutions has been questioned recently by Dean *et al.*<sup>24</sup> It seems more appropriate in view of the large numbers of ambiguous solutions and the vagaries of the shortest-path method to consider energy-dependent analyses. Several such analyses have been done in the past.<sup>8</sup> A recent analysis which includes for the first time the results of this experiment has been carried out by Arndt *et al.*<sup>12</sup> In this analysis the energy-dependent partial-wave amplitudes used to fit the data have the property that they can be analytically continued to possible resonance poles.

It seems that this might be a better way to search for the  $Z_1^*$ , since in the conventional analysis in which one examines the Argand trajectory, a broad inelastic resonance is difficult to see in the presence of an energy-dependent nonresonant background.<sup>25</sup> A very good fit with  $\chi^2/\text{NDF} = 1.33$  was obtained using 42 parameters based on the  $l \leq 4$  partial waves. The Argand trajectories of the lower partial waves are shown in Fig. 8, in which the speeds can be estimated by the markings at fixed 100-MeV/c intervals of laboratory momentum. A resonance pole was found in the  $P_{3/2}$  partial-wave amplitude with mass coordinates  $M_z - i\Gamma/2 = (1787 - i100)$  MeV. Various altered forms of the analysis were attempted, each producing a pole at about the above coordinates.

#### ACKNOWLEDGMENTS

We wish to thank the ANL-ZGS staff for their valuable assistance and support during the course of this experiment. We also extend our thanks to Mr. F. Desrosier and the University of Maryland Machine Shop for their assistance in the design and construction of much of the experimental apparatus.

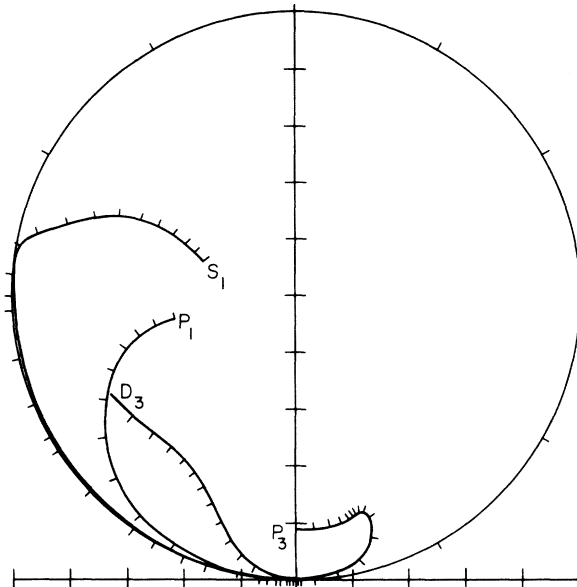


FIG. 8. Argand diagrams of the dominant partial-wave amplitudes from the phase-shift analysis of Arndt *et al.* (Ref. 12). The markings define 100 MeV/c intervals of constant laboratory momentum up to 2.0 GeV/c.

†This work was supported in part by the U. S. Atomic Energy Commission.

\*Present address: Rutgers University, New Brunswick, New Jersey.

‡Present address: New York University, New York, N. Y.

§Present address: Purdue University, W. Lafayette, Indiana.

<sup>1</sup>O. W. Greenberg and M. Resnikoff, Phys. Rev. 163, 1844 (1967).

<sup>2</sup>H. Harari, in *Proceedings of the Fourteenth International Conference on High Energy Physics, Vienna, 1968*, edited by J. Prentki and J. Steinberger (CERN, Geneva, 1968), p. 195.

<sup>3</sup>P. G. O. Freund, Phys. Rev. Lett. 20, 235 (1968); H. Harari, *ibid.* 20, 1395 (1968).

<sup>4</sup>O. B. Chiu and J. Finkelstein, Phys. Lett. 27B, 510 (1968). See also J. Mandula, J. Weyers, and G. Zweig, Phys. Rev. Lett. 23, 266 (1969); J. Mandula, C. Rebbi, R. Slansky, J. Weyers, and G. Zweig, Phys. Rev. Lett. 22, 1147 (1969).

<sup>5</sup>J. Rosner, Phys. Rev. Lett. 21, 950 (1968).

<sup>6</sup>Stanley Mandelstam, Phys. Rev. D 1, 1735 (1970).

<sup>7</sup>R. L. Cool, G. Giacomelli, T. F. Kycia, B. A. Leontic, K. K. Li, A. Lundby, J. Teiger, and C. Wilkin, Phys. Rev. D 1, 1887 (1970); D. V. Bugg, R. S. Gilmore, K. M. Knight, D. C. Salter, G. H. Stafford, E. J. N. Wilson, J. D. Davies, J. D. Dowell, P. M. Hattersley, R. J. Homer, A. W. O'Dell, A. A. Carter, R. J. Tapper, and K. F. Riley, Phys. Rev. 168, 1466 (1968); T. Bowen, P. I. Caldwell, F. Ned Dikman, E. W.

Jenkins, R. M. Kalbach, D. V. Petersen, and A. E. Pifer, Phys. Rev. D 2, 2599 (1970); T. Bowen, E. W. Jenkins, R. M. Kalbach, D. V. Petersen, A. E. Pifer, and P. K. Caldwell, *ibid.* 7, 22 (1973); A. S. Carroll, T. F. Kycia, K. K. Li, D. N. Michael, P. M. Mockett, D. C. Rahm, and R. Rubenstein, Phys. Lett. 45B, 531 (1973).

<sup>8</sup>A review of  $KN$  partial-wave analysis is given in Particle Data Group, LBL Report No. LBL-100, 1974 (unpublished).

<sup>9</sup>K. Abe, B. A. Barnett, J. H. Goldman, G. J. Marmer, D. R. Moffett, and E. F. Parker in *Baryon Resonances-73*, proceedings of the Purdue Conference on Baryon Resonances, edited by E. C. Fowler (Purdue Univ. Press, Lafayette, Indiana, 1973).

<sup>10</sup>K. Abe, B. A. Barnett, J. H. Goldman, A. T. Laasanen, P. H. Steinberg, G. J. Marmer, D. R. Moffett, and E. F. Parker, Phys. Rev. D 10, 3556 (1974).

<sup>11</sup>J. H. Goldman, Ph.D. thesis, Univ. of Maryland Report No. 73-054, 1972 (unpublished).

<sup>12</sup>R. A. Arndt, R. H. Hackman, L. D. Roper, and P. H. Steinberg, Phys. Rev. Lett. 33, 987 (1974).

<sup>13</sup>B. A. Barnett, A. T. Laasanen, P. F. M. Koehler, P. H. Steinberg, J. G. Asbury, J. D. Dowell, D. Hill, S. Kato, D. Lundquist, T. B. Novey, A. Yokosawa, G. Burleson, D. Eartly, and K. Pretzl, Phys. Rev. D 8, 2751 (1973).

<sup>14</sup>B. J. Charles, I. M. Cowan, T. R. M. Edwards, W. M. Gibson, A. R. Gillman, R. S. Gilmore, M. H. Gledhill, C. M. Hughes, J. Malos, V. J. Smith, R. J. Tapper, B. McCartney, D. L. Ward, P. D. Wroath, G. A. Beck,

- M. Coupland, and S. G. F. Frank, Rutherford Laboratory Report No. RPP/H/95 (unpublished).
- <sup>15</sup>Values of  $d\sigma/d\Omega(0)$  from the Legendre polynomial fitting are on the average 2% below the values given in the table.
- <sup>16</sup>J. A. Danysz, D. K. Pennery, B. C. Stewart, G. Thompson, J. M. Brunet, J. L. Narjoux, J. E. Allen, N. J. D. Jacobs, P. H. Lewis, and P. V. March, Nucl. Phys. B42, 29 (1972).
- <sup>17</sup>G. Giacomelli, P. Lugaresi-Serra, G. Madrioli, A. M. Rossi, F. Griffiths, I. S. Hughes, D. A. Jacobs, R. Jennings, B. C. Wilson, G. Ciapetti, V. Constantini, G. Martellotti, D. Zanello, E. Castelli, and M. Sessa, Nucl. Phys. B20, 301 (1970).
- <sup>18</sup>P. Baillon, C. Bricman, M. Ferro-Luzzi, J. M. Perreau, R. D. Tripp, T. Ypsilantis, Y. Déclais, and J. Séguinot, Phys. Lett. 50B, 383 (1974).
- <sup>19</sup>P. Baillon, C. Bricman, M. Ferro-Luzzi, J. M. Perreau, R. D. Tripp, T. Ypsilantis, Y. Déclais, and J. Séguinot, Phys. Lett. 50B, 377 (1974).
- <sup>20</sup>The methods employed in the phase-shift analysis are described in University of Maryland Report No. 70-101 (unpublished).
- <sup>21</sup>S. Kato, P. Koehler, T. Novey, A. Yokosawa, and G. Burleson, Phys. Rev. Lett. 24, 615 (1970).
- <sup>22</sup>F. C. Erne, J. C. Sens, and F. Wagner, in *Hyperon Resonances—70*, edited by Earl C. Fowler (Moore, Durham, N. C. 1970).
- <sup>23</sup>C. Lovelace and F. Wagner, Nucl. Phys. B28, 141 (1971).
- <sup>24</sup>N. W. Dean, T. C. Jensen, and W. F. Long (unpublished).
- <sup>25</sup>R. Ayed, P. Bareyre, J. Feltesse, and G. Villet, Phys. Lett. 32B, 404 (1970).